Journal of **N**onlinear **A**nalysis and **O**ptimization
Vol. 14, Issue. 1 : 2023
ISSN : **1906-9685**

UTILIZING SPIN-TORQUE TO TOGGLE NON-COLLINEAR ANTIFERROMAGNETIC ANTIPEROVSKITES

[#1]Mr.AMMASI THIRUGNANAM, *Assistant Professor*
[#2]Mrs.BEERAM JAMUNA, *Assistant Professor*
Department of Physics,
SREE CHAITANYA INSTITUTE OF TECHNOLOGICAL SCIENCES, KARIMNAGAR, TS.

ABSTRACT: The Néel vector is used as a state variable in AFM spintronics to construct new electrical devices. A intriguing new study shows that a spin-orbit force can change the phase of the Néel vector. Nonetheless, collinear antiferromagnets with the proper magnetic space-group symmetry are the primary research focus. Nonetheless, for this type of switching application, a wide range of high-temperature noncollinear antiferromagnets are accessible. Spin torque, according to this article, can efficiently change the noncollinear antiferromagnetic (AFM) order of antiperovskite materials. Using atomistic spin-dynamics modeling and first-principles computations, we show that the antiferromagnetic (AFM) order in antiperovskites ANMn3 (where A can be Ga, Ni, etc.) can change very quickly, in picoseconds, up to the 4g ground state. This is performed by the use of a spin force, which is generated by a spin current. The threshold switching current density can be changed by altering the ANMn3 stoichiometry engineering and magnetocrystalline anisotropy. The 4g antiferromagnetic (AFM) phase produces a characteristic anomalous Hall effect, which can be used to identify the spin-torque switching of the AFM order. Because of their capacity to quickly swap modes and select the appropriate one, antiferromagnetic (AFM) spintronics holds enormous promise for noncollinear magnetic antiperovskites as a material platform.
Key words: Spin-torque switching,Noncollinear antiferromagnetism,Spintronics.

AFM spintronics is a relatively young field. The AFM order element Néel vector modifies the spin-dependent transport properties. This is the objective. Antiferromagnets could be used instead of ferromagnets in spintronic devices that store and process data. These magnets are fast, have no stray magnetic fields, and can withstand magnetic shocks. To realize this potential, new methods for storing and decoding AFM Néel vector information are required. Because antiferromagnets lack universal magnetism, this is more difficult to achieve than with ferromagnetic materials.

According to a new study, passing an electric current through a solid collinear antiferromagnet with a specific magnetic group symmetry can change the AFM Néel vector. The inverse spin galvanic effect produces a field-like spin force on specific sublattices in antiferromagnets such as Mn2Au and CuMnAs. Despite breaching space-inversion symmetry, these antiferromagnets can create space-inversion partners [6-8]. When an electric current passes a certain threshold, the Néel vector changes . In bilayer heterostructures such as NiO/Pt and Mn2Au/Pt the spin-Hall effect facilitates Néel vector switching. A spin current enters the system, creating a spin force that acts as an antidamping force. In these materials, anisotropic magnetoresistance (AMR) or spin-Hall magnetoresistance (SMR) effects are frequently utilized to determine the AFM Néel vector. Because of their minimal affects, these devices' size and readout speed can only be reduced so much—usually less than 1%. High writing currents and heat from Néel vector flips may have generated some magnetoresistive phenomena. AFM order parameters could be identified via the

anomalous Hall effect (AHE). Noncollinear antiferromagnetic (AFM) materials are used. They may be able to replace their classmates. Mn3X (X Ga, Zn, Ag, or Ir) and ANMn3 (A Ga, Zn, Ag, or Ni) are noncollinear antiferromagnets with high anomalous Hall conductivities (AHC). The anomalous Hall effect (AHE) should be shifted if the Néel vectors of these molecules are rotated. Even though the AHE lacks time-reversal symmetry, we may calculate the antiferromagnetic (AFM) order using normal Hall measurements.

The spin torque of these noncollinear antiferromagnets can change the order of the AFM structure. The addition of a spin current can change the magnetic configuration of a noncollinear antiferromagnet dynamically. In a two-dimensional model with a single Kagomé layer, spin-transfer torque can change the spin arrangement of a chiral antiferromagnet. According to a new study, adding a spin current perpendicular to the plane of a triangle construction could translate the domain wall of a 4g-type antiferromagnet. These modeling studies help us understand how the magnetization of noncollinear antiferromagnets varies as they are pushed by spin-torque. Regardless, a valuable AFM description

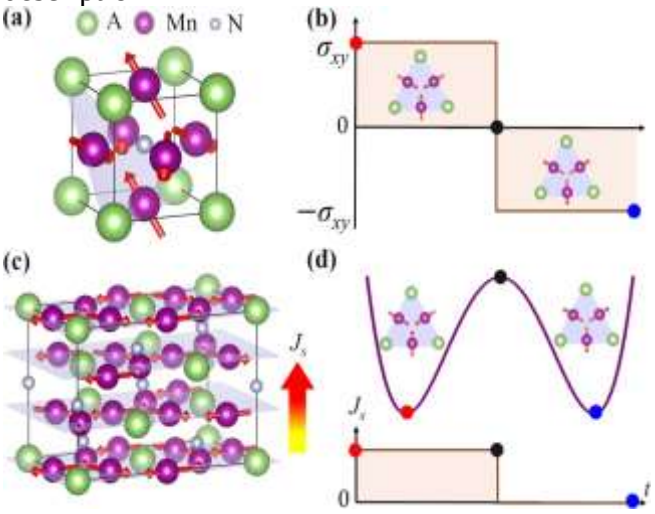

FIG. 1. ANMn3 antiperovskite's noncollinear AFM 4g state is found in cubic unit cells. Manganese magnetic directions are indicated by red lines. Because of antiferromagnetic order flipping, the unique Hall conductivity xy rotates. The magnetic structure of ANMn3 is depicted in the plane insets. The orthorhombic supercell of ANMn3 is used to model spin dynamics. A spin current Js along the axis causes a spin torque on the magnetic moments of ANMn3. d) Rotation causes the order switching mechanism of the AFM to shift. According to first-principles calculations, the examined antiferromagnets do not have enough spin torque to change magnetic order. Using DFT calculations, atomistic spin-dynamics modeling, and the Landau-Lifshitz Gilbert-Slonczewski (LLGS) equation [36], we show that spin torque impacts the non-collinear antiferromagnetic (AFM) order in antiperovskite materials. In ANMn3 materials, we show that a spin current can rapidly change the antiferromagnetic (AFM) ordering of the 4g ground state. Ga, Ni, and other A-containing compounds are currently being researched. By varying magnetocrystalline anisotropy, ANMn3 stoichiometry engineering can alter the threshold switching current density. The AFM order spin-torque reversal can be discovered by investigating the unique Hall effect in references 37-47. Figure 1a depicts the opposing cation and anion configurations of antiperovskite molecules. The AXM3 family of 3D transition-metal intermetallic compounds is one of the most investigated antiperovskite families. This family is made up of A from the main group, X (carbon or nitrogen), and M (a 3/4 transition metal). ANMn3 is an antiperovskite nitride with Mn as the parent and A as the replacement, unlike Ga, Ni, Cu, Zn, and others. This is due to mismatched magnetic moments in AFM phases. Every Mn magnetic moment in the plane rotates 90°, which is especially noticeable in 4g (see Fig. 1(a)) and 5g. These magnetic characteristics are produced by AFM coupling in the plane frustrated Kagomé lattice. Non-aligned AFM couplings can accomplish magnetoelectric, magnetocaloric, and piezoelectric functionalities.

AHE was recently discovered in antiperovskite nitrides containing Mn and 4g AFM. This was predicted by theory and supported by real-world evidence.To modify the anomalous Hall effect (AHE) direction in 4g-type antiperovskites, the AFM order must be changed. The time-reversal symmetry process, as shown in Figure 1(b), causes the anomalous Hall conductivity (AHC) to appear strange. This approach effortlessly

distinguishes between the two AFM states that 4g-phase molecules can inhabit. By developing a way to flip between the two AFM states in 4g molecules, the AHE readout may shed light on a potential AFM spintronics path.

We investigate how spin-torque impacts the antiferromagnetic (AFM) order of these compounds. They are 4g noncollinear antiferromagnetic antiperovskite. The plane is used to layer the antiperovskite thin film. Nonlinear antiferromagnetic exchange coupling aligns Mn magnetic moments in this plane. In Figure 1(c), magnetic fluctuations are created by injecting a spin current Js in the direction of In addition to the spin-Hall effect, an adjacent heavy metal or ferromagnetic layer can generate a spin-polarized charge current that transfers the spin current. By creating spin, the spin current Js generates a moment in the Mn magnetic plane. The LLGS equation governs the temporal evolution of magnetism.

$$\frac{\partial \vec{m}_i}{\partial t} = -\gamma(\vec{m}_i \times \vec{H}_i) + \alpha_G\left(\vec{m}_i \times \frac{\partial \vec{m}_i}{\partial t}\right) + \gamma\left(\vec{m}_i \times \vec{H}_i^s\right). \quad (1)$$

Here α_G is the Gilbert damping constant, γ is the gyromagnetic ratio, $\vec{m}_i = \frac{\vec{M}_i}{|M_i|}$ is the unit magnetization vector for each sublattice with the magnetization $\vec{M}_i$. The magnetic field $\vec{H}_i = -\frac{1}{\mu}\frac{\partial H}{\partial \vec{m}_i}$ is determined by the spin Hamiltonian:

$$H = -\sum_{i \neq j} J_{ij}\vec{m}_i \cdot \vec{m}_j - K\sum_i (\hat{n}_i \cdot \vec{m}_i)^2, \quad (2)$$

where μ is the magnetic moment of a Mn atom, J_{ij} is the exchange coupling energy between sublattices, K is the magnetic anisotropy energy per Mn atom, and $\hat{n}_i$ is the direction of the easy axis for each sublattice. $\vec{H}_i^s = h_s(\vec{m}_i \times \vec{p}_s)$ is the effective magnetic field produced by the spin current J_s with the spin polarization along the $\vec{p}_s$ direction. The coefficient h_s is given by $h_s = \frac{\hbar J_s}{eLM}$, where $M = |\vec{M}_i|$ is the magnitude of the sublattice magnetization, e is the electronic charge, $\hbar$ is the Planck's constant, L is thickness of the sample. This effective field generates the spin torque $\sim \vec{m}_i \times \vec{H}_i^s$, which drives the magnetization dynamics.

The AFM sequence can be inverted to provide a 180° rotation of each moment inside the horizontal plane [Fig. 1(d)]. The induced out-of-plane field is as follows when aligned parallel to the plane: $\vec{H}_i^s$

I intend to correct the incongruent times. Antiferromagnetic (AFM) materials naturally exchange moments, resulting in an additional magnetic component in the same direction. As a result, the energy profile becomes less favorable. However, if it is heading in an aileron direction,, i.e., $\vec{p}_s = \hat{z}$, the induced field

$\vec{H}_i^s = h_s(\vec{m}_i \times \hat{z})$

Runs parallel to and at a right angle to the orientation inside the same plane [as illustrated by black arrows in Figure 2(a)]. The staggered field Hsi causes nearly equal rotation of magnetic moments in three sublattices while having little effect on the remaining twelve.

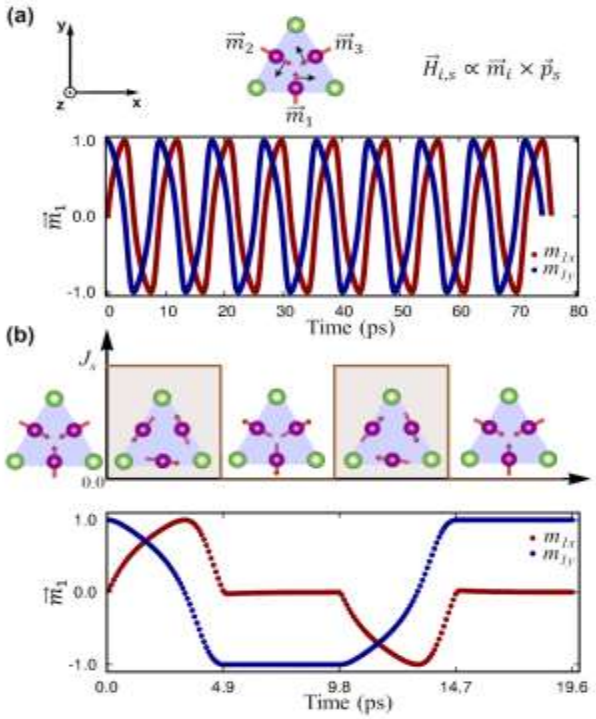

FIG. 2. Spin dynamics in antiperovskite $NiNMn_3$. (a) Top panel: schematic of effective magnetic field $\vec{H}_i^s$ (black arrows) on the three sublattices $\vec{m}_1$, $\vec{m}_2$, and $\vec{m}_3$ generated by spin current J_s with the spin polarization $\vec{p}_s$ along the z direction. Bottom panel: time-dependent variations of the x- and y components of $\vec{m}_1$ during the application of spin current $J_s = 1.8 \times 10^{12}$ A/m^2. (b) Top panel: schematic of the spin-torque switching process induced by two spin-current pulses. Bottom panel: time-dependent variations of the x- and y components of $\vec{m}_1$ driven by applying the two spin-current pulses of 4.9 ps in duration.

Shifting is preferable because there are no energy exchange prices. This scenario examines spin-torque switching, which occurs when the spin current Js causes spin polarization to travel parallel to z. On an ANMn3 slab, atomistic simulation spin-torque dynamics were performed (Fig. 1(c)). The repeating supercells made up the 6 nm-thick slab. We are particularly interested in

NiNMn3, a metal antiperovskite discovered lately at room temperature using AFM order and a sustained AHE effect. According to our DFT model, NiNMn3 has the least energy in the magnetic state with the lowest net magnetization. DFT was used to calculate the NiNMn3 characteristics of Equation (2). There were no Ni atoms with a local magnetic moment of 2.7614B, whereas all Mn atoms did. Using energy-mapping, the exchange constant Ji j is -24 meV. The structure rotates 90 degrees when all magnetic moments are rotated 180 degrees around the axis. Because of magnetic anisotropy, this spinning has higher energy (Figure 1(d)). The magnetic anisotropy constant K can be calculated using the energy difference between phases. (E5g E4g)/3, or 0.03 meV per Mn atom, is the difference. They are 63 and 64 years old, respectively. For identical noncollinear magnets, the experimental damping constant G is 0.05-0.28. We employ a gyromagnetic ratio of 1.76 1011 T1 s1 and G = 0.1 in our computations. The initial magnetic configuration is shown in Figure 2(a) (top panel), in which the three sublattices align with the center point of the triangle formed by the nearest Mn atoms. We monitor the change in m1, which has a starting x component of 0 (m1x) and a maximum y component of 1 to track the simulated spin-torque switching process. The spin torque from Js = 1.8 1012 A/m2 spins it, as shown in Figure 2(a) (bottom panel). When the current flows, M1x and M1y oscillate clockwise, suggesting that moments are moving clockwise. Rf and observed fluctuation frequency quality are similar. Waves last 9.8 picoseconds, or 0.1 terahertz. . Because Jc is the critical current density, f = 1/4 3 Js Jc 3K G makes sense. The operation of AFM may have an impact on the design of small generators that emit regulated Terahertz radiation. Any number between 65 and 67 is acceptable. These engines are required by many technologies. After a 4.9-picosecond spin-current pulse, moments rotate 180 degrees. When the initial magnetic configuration of NiNMn3 is pulsed, the three Mn magnetic moments—m1, m2, and m3—move from the center to the edges of the triangle formed by the nearest Mn atoms, as shown in Figure 2(b). At 5g, middle-phase magnetic moments collide inside a vortex. The packing and relocating process has begun. A 4.9-picosecond pulse is used to reestablish the magnetic structure. The results indicate that spin-torque can rapidly modify the AFM order in NiNMn3. Spin currents are caused by charge currents that initiate the spin-Hall effect or spin-polarized charge currents. Reduced charge current density and spin-torque shift Js minimize Joule heat and energy consumption. Anisotropic energy has the greatest impact on Js [33,68]. When hs > K, the Zeeman energy (hs) of the magnetic moment in the effective field (Hsi) induced by Js must surpass the anisotropy energy (K). This is required to change the magnetic orientations of Mn. Jc denotes the critical current density and KLe hV3 denotes the NiNMn3 cubic unit cell volume. Jc's result corresponds to Reference [33]. Because Jc is directly related to K, decreasing magnetic anisotropy reduces critical current density. This is supported by our atomistic simulation of NiNMn3's spin-torque switching. The magnetic anisotropy constant K is changed but not the others. As seen in Figure 3(a), decreasing k yields the

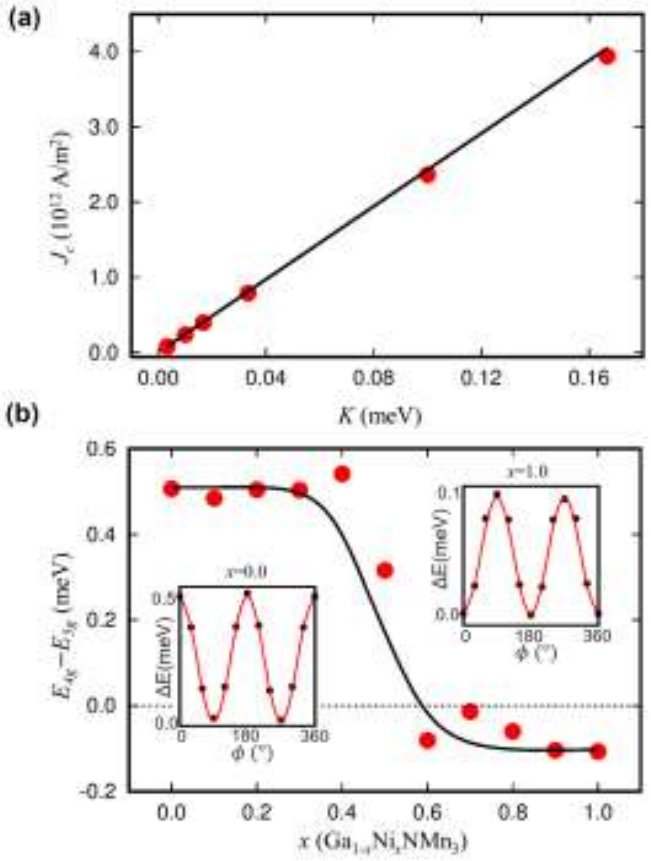

FIG. 3. (a) Critical current density J_c for switching of the AFM order in $ANMn_3$ antiperovskite as a function of the anisotropy energy. The red dots are J_c obtained by the atomistic spin dynamics modeling. The solid black line is obtained from $J_c = \frac{\Delta E_a}{N\hbar}$. (b) The energy difference between the Γ_{4g} and Γ_{5g} magnetic configurations in $Ga_{1-x}Ni_xNMn_3$. The insets show the energy as a function of rotation angle ϕ of the magnetic moments around the [111] axis in $Ga_{1-x}Ni_xNMn_3$ for $x = 0$ ($GaNMn_3$) and $x = 1$ ($NiNMn_3$), where $\Delta E = E_{4g} - E(\phi)$.

The decrease in Jc occurs in a straight line. Setting the anisotropy constant K to 0.01 meV per Mn atom appears to reduce the critical current density Jc to around 1010 A/m2. The solid line in Figure 3(a) demonstrates that the computed critical current density (Jc) is the same as the fundamental estimate (KLe hV3). Chemical modifications can alter an antiperovskite's magnetic field. GaNMn3 is one of the antiferromagnetic 5g order perovskites. As a result, it is envisaged that a doped Ga1xNixNMn3 molecule will exhibit the ground 5g state in Ga-rich phases and the 4g state in Ni-rich phases. There should be a crossover point at doping level x where there is no longer any magnetic anisotropy between the two phases. Figure 3(b) depicts the energy difference between the 5g and 4g magnetic arrangements, where x represents the degree of doping. The estimated ground states for GaNMn3 (x = 0) and NiNMn3 (x = 1) are 5g and 4g, respectively, which are consistent with the experimental results. There is a transition between the two stages when x is smaller than 0.58. The magnetic anisotropy is substantially smaller in this area, and

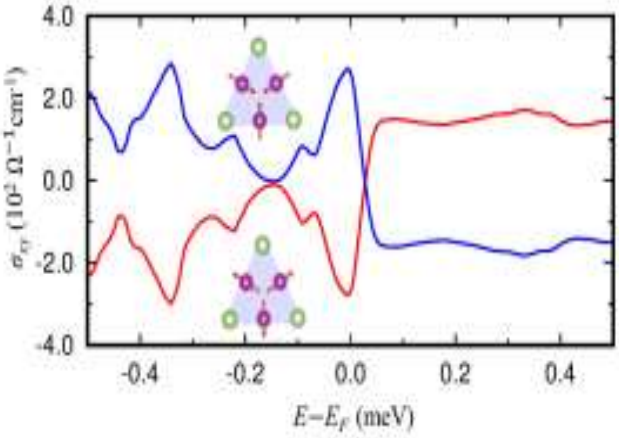

FIG. 4. Calculated anomalous Hall conductivity (AHC)σ_{xy} of antiperovskite $Ga_{0.42}Ni_{0.58}NMn_3$ with the AFM Γ_{4g} order as a function of energy. The red and blue lines denote the AHC for the two AFM states with reversed magnetic structure shown in the insets.

The critical current density for AFM order spin-torque switching is expected to be around 1010 A/m2. The peculiar Hall conductivity can be used to identify the transitioning of the antiferromagnetic (AFM) order in the 4g phase

$$\sigma_{\alpha\beta} = -\frac{e^2}{\hbar}\int_{BZ}\frac{d^3\vec{k}}{(2\pi)^3}\Omega_{\alpha\beta}(\vec{k}), \qquad (3)$$

$$\sigma_{\alpha\beta} = -\frac{e^2}{\hbar}\int_{BZ}\frac{d^3\vec{k}}{(2\pi)^3}\Omega_{\alpha\beta}(\vec{k}), \qquad (3)$$

where $\Omega_{\alpha\beta} = \sum_n f_n(\vec{k})\Omega_{n,\alpha\beta}(\vec{k})$ is the sum of the Berry curvatures $\Omega_{n,\alpha\beta}(\vec{k})$ corresponding the individual bands n, $f_n(\vec{k})$ is the Fermi distribution function, and indices (α, β) denote Cartesian coordinates. The expression for the Berry curvature $\Omega_{n,\alpha\beta}(\vec{k})$ is given by [20,69]

$$\Omega_{n,\alpha\beta}(\vec{k}) = -2i\hbar^2\sum_{m\neq n}\frac{\langle\psi_{n,\vec{k}}|v_\alpha|\psi_{m,\vec{k}}\rangle\langle\psi_{m,\vec{k}}|v_\beta|\psi_{n,\vec{k}}\rangle}{(E_m(\vec{k}) - E_n(\vec{k}))^2}, \qquad (4)$$

where $\psi_{n,\vec{k}}$ is the Bloch function and $\vec{v}$ is the velocity operator. The Berry curvature is odd under certain symmetry operations, i.e., $\hat{O}\Omega_n(\vec{k}') = -\Omega_n(\vec{k})$, where $\hat{O}$ is a symmetry operation such as time-reversal symmetry or mirror

$$\sigma_{\alpha\beta} = -\frac{e^2}{\hbar}\int_{BZ}\frac{d^3k}{(2\pi)^3}\Omega_{\alpha\beta}(\vec{k}), \quad (3)$$

where $\Omega_{\alpha\beta} = \sum_n f_n(\vec{k})\Omega_{n,\alpha\beta}(\vec{k})$ is the sum of the Berry curvatures $\Omega_{n,\alpha\beta}(\vec{k})$ corresponding the individual bands n, $f_n(\vec{k})$ is the Fermi distribution function, and indices (α, β) denote Cartesian coordinates. The expression for the Berry curvature $\Omega_{n,\alpha\beta}(\vec{k})$ is given by [20,69]

$$\Omega_{n,\alpha\beta}(\vec{k}) = -2i\hbar^2\sum_{m\neq n}\frac{\langle\psi_{n,\vec{k}}|v_\alpha|\psi_{m,\vec{k}}\rangle\langle\psi_{m,\vec{k}}|v_\beta|\psi_{n,\vec{k}}\rangle}{(E_m(\vec{k}) - E_n(\vec{k}))^2}, \quad (4)$$

where $\psi_{n,\vec{k}}$ is the Bloch function and $\vec{v}$ is the velocity operator. The Berry curvature is odd under certain symmetry operations, i.e., $\hat{O}\Omega_n(\vec{k}') = -\Omega_n(\vec{k})$, where $\hat{O}$ is a symmetry operation such as time-reversal symmetry or mirror

There is mirror and time-reversal symmetry [69, 70]. Odd n values are forbidden in the 4g AFM state since there is no symmetry operation O that performs this. When Equation (4) returns a non-zero value, the Hall effect occurs. Figure 4 depicts the energy dependence of Ga1xNixNMn3's predicted AHC xy, with an emphasis on x at 0.58. Fermi energy is represented by the symbol xy = 261 cm1. Magnetic moments rotate about the axis, causing the magnetic band structure and space group to change. As a result, xy changes. When the moments are aligned in the 5g state, Xy declines until it reaches zero, as shown in Supplementary Material. From their 4g position, they rotate. When the AFM is inverted, the AHC changes signals, as seen in Figure 4. When antiperovskite ANMn3 sheets are inserted in the plane opposing , the AFM order changes. In a non-collinear AFM state, spin-torque switching is possible if the spin-polarization component of the spin current is not parallel to the plane. Spin currents are generated in nonmetallic bottom layers by the spin-Hall effect. Spin-hall torque switching was reported in the GaNMn3 (001)/Pt bilayer structure in a recent work. This work discovered that the noncollinear antiferromagnetic (AFM) 5g phase of Mn3GaN suppresses the anomalous Hall effect. employed the normal anisotropic magnetoresistance (AMR) phenomenon to identify AFM switching. Our results reveal that anisotropic Hall conductivity (AHC) sign shift in noncollinear antiferromagnetic (AFM) antiperovskites with the AFM 4g phase is helpful to order. This is distinct from the AMR and SMR measurement methods. In AFM, antiperovskite nitrides containing Mn, such as NiNMn3, may switch spin torque nonlinearly. This concept reflects the finished product. We obtained a realistic spin-current density to demonstrate that this transition can take place in picoseconds. The stoichiometry can be changed to adjust the magnetocrystalline anisotropy and AFM switching current density. The antiperovskite compound Ga1xNixNMn3 was investigated, with x about 0.58. The compound exhibits an anomalous Hall conductivity (xy) of 260 1 cm1 and a critical spin-current density (Jc) of 1010 A/m2. The AFM commands can be identified by examining the characteristic Hall conductivity shift that occurs when the AFM is turned on and off. We anticipate that the quality of spintronic devices will improve over time. To regulate and localize the AFM order, the material framework employs noncollinear AFM antiperovskites. The NSF funded the project through Nebraska MRSEC (Grant No. DMR 1420645) and DMREF (Grant No. DMR-1629270). The study was done by the University of Nebraska's Holland Computing Center. GNUPLOT and VESTA were used to do the calculations.

CONCLUSION

In conclusion, the exploration of spin-torque switching in noncollinear antiferromagnetic antiperovskites marks a significant leap forward in the field of spintronics and magnetism. The discovery of the unique properties of these materials has opened doors to novel mechanisms for manipulating magnetic moments, offering potential breakthroughs in data storage and information processing technologies.

The ability to control the orientation of the antiferromagnetic order through spin-torque effects introduces exciting prospects for low-energy, high-speed data writing and processing. This phenomenon not only showcases the intricate interplay between spin currents and noncollinear magnetic structures but also demonstrates the promise of antiferromagnetic materials in advancing spintronic applications.

However, despite these promising findings, there are challenges to overcome, including optimizing material properties, enhancing efficiency, and ensuring stability at ambient conditions. Further research is crucial to fully

understand the underlying physics, improve control mechanisms, and scale up these materials for practical device applications.

Collaborations across disciplines, from theoretical physics to materials science and engineering, will be instrumental in addressing these challenges and realizing the potential of spin-torque switching in noncollinear antiferromagnetic antiperovskites. With continued exploration and innovation, these materials could revolutionize the landscape of spintronics, paving the way for more efficient and versatile next-generation electronic devices.

REFERENCE

1. T. Jungwirth, X. Marti, P. Wadley, and J. Wunderlich, Antifer- romagnetic spintronics, Nat. Nanotechnol. 11, 231 (2016).
2. V. Baltz, A. Manchon, M. Tsoi, T. Moriyama, T. Ono, and Y. Tserkovnyak, Antiferromagnetic spintronics, Rev. Mod. Phys. 90, 015005 (2018).
3. T. Jungwirth, J. Sinova, A. Manchon, X. Marti, J. Wunderlich, and C. Felser, The multiple directions of antiferromagnetic spintronics, Nat. Phys. 14, 200 (2018).
4. P. Wadley, B. Howells, J. Železný, C. Andrews, V. Hills, R. P. Campion, V. Novák, K. Olejník, F. Maccherozzi, S. S. Dhesi, S. Y. Martin, T. Wagner, J. Wunderlich, F. Freimuth, Y. Mokrousov, J. Kuneš, J. S. Chauhan, M. J. Grzybowski, A. W. Rushforth, K. W. Edmonds, B. L. Gallagher, and T. Jungwirth, Electrical switching of an antiferromagnet, Science 351, 587 (2016).
5. S. Y. Bodnar, L. Šmejkal, I. Turek, T. Jungwirth, O. Gomonay, J. Sinova, A. A. Sapozhnik, H.-J. Elmers, M. Kläui, and M. Jourdan, Writing and reading antiferromagnetic Mn_2Au by Néel spin-orbit torques and large anisotropic magnetoresis- tance, Nat. Commun. 9, 348 (2018).
6. J. Železný, H. Gao, K. Výborný, J. Zemen, J. Mašek, Manchon, J. Wunderlich, J. Sinova, and T. Jungwirth, Relativistic Néel-Order Fields Induced by Electrical Cur- rent in Antiferromagnets, Phys. Rev. Lett. 113, 157201 (2014).
7. J. Železný, H. Gao, A. Manchon, F. Freimuth, Y. Mokrousov, J. Zemen, J. Mašek, J. Sinova, and T. Jungwirth, Spin-orbit torques in locally and globally noncentrosymmetric crystals: Anti-ferromagnets and ferromagnets, Phys. Rev. B 95, 014403 (2017).
8. Manchon, J. Zelezný, I. M. Miron, T. Jungwirth, J. Sinova, Thiaville, K. Garello, and P. Gambardella, Current-induced spin-orbit torques in ferromagnetic and antiferromagnetic sys- tems, Rev. Mod. Phys. 91, 035004 (2019).
9. X. Z. Chen, R. Zarzuela, J. Zhang, C. Song, X. F. Zhou, G. Y. Shi, F. Li, H. A. Zhou, W. J. Jiang, F. Pan, and Y. Tserkovnyak, Antidamping Torque-Induced Switching in Biaxial Antiferro-magnetic Insulators, Phys. Rev. Lett. 120, 207204 (2018).